



SEISMIC VULNERABILITY OF RC WITH INFILLS SCHOOL BUILDINGS IN EL SALVADOR, A DETAILED ASSESSMENT.

M. Lopez⁽¹⁾, J. Hernández⁽²⁾

⁽¹⁾ Professor, Universidad de El Salvador, manuel.lopez@fia.ues.edu.sv

⁽²⁾ Doctoral candidate, Universidad de El Salvador, jaimepaz@fia.ues.edu.sv

...

Abstract

With a geographical extension of a little more than 20,000 km², and a population of about 6,000,000 inhabitants, the republic of El Salvador is struck by a destructive earthquake, or earthquake sequence, once per decade on average. The frequency of damaging earthquakes clearly demonstrates that El Salvador is a country of very high seismic hazard. Indeed, the capital city, San Salvador, is probably the city in the Americas that has been most frequently damaged by earthquakes. The most recent earthquake sequence, in 2001, caused more than 1,000 deaths all over the country and more than 210 million dollars in losses in the education sector.

In a recent project funded by the World Bank, as part of the Global Program for Safer Schools (GPSS), which is an initiative of the Global Facility for Disaster Reduction and Recovery (GFDRR), which seeks to make schools more resilient to natural disasters; it was found the portfolio of education in El Salvador comprises 15430 school buildings allocated in 6078 educative centers, where 13412 buildings belong to the public sector whilst the rest to private institutions. One of the key elements to assess the seismic risk in the education portfolio is the fragility/vulnerability curves. The reinforced concrete frames with masonry infill school buildings, most of which were built after the 2001 earthquakes and designed with the current seismic code of 1997, was one of the structural typologies found and to which these curves were computed.

This research is one of the first to use Incremental Dynamic Analysis to develop fragility/vulnerability curves for a Salvadoran structural typology and to provide important damage probability parameters, as well. In addition, within the GPSS project, the fragility and vulnerability curves calculated will become a part of the Global Library of Scholar Infrastructure (GLoSI) of the World Bank. Furthermore, the information obtained from this research could be used towards the development of uniform risk maps in El Salvador.

Keywords: fragility curves, vulnerability curves, schools, risk analysis, El Salvador



1. Introduction

Risk analysis and assessment of building population is a quite new subject applied in El Salvador. In the present case, the development of fragility and vulnerability curves of a specific type of educational building is explained, the product of which was used in the risk assessment of the education portfolio of El Salvador.

2. Index buildings

The Education portfolio of El Salvador has 6078 school centers with 15430 buildings, 13412 of which belong to the public sector. Table 1 shows the distribution of the school buildings of the public sector classified by construction type. Note that this categorization is based on the Global Program for Safer Schools (GPSS) Taxonomy guide adapted to the El Salvador case.

Table 1 – Public school buildings classified by construction type

Structural typology	Code	# of schools	%
Adobe (A)	A	34	0.3%
Unreinforced masonry (UCM/URM)	UCM/URM6	31	0.2%
Confined masonry	CM	5529	41.2%
Reinforced masonry	RM	3663	27.3%
Both directions: RC frame with Masonry Walls without seismic gap (fully integrated). Without short column geometry	RC1	93	0.7%
Both directions: RC frame with Masonry Walls without seismic gap with short column geometry	RC2	22	0.2%
RC1 frame in one direction and RC2 in the other direction	RC3	496	3.7%
Both directions: RC frame with Masonry Walls with seismic gap enough to prevent interaction	RC4	129	1.0%
RC1 frame in one direction and RC4 in the other direction	RC5	14	0.1%
RC dual systems	RCD	3	0.0%
Reinforced concrete structural walls	RCW	2	0.0%
Precast	RPS	51	0.4%
Steel frames	SF1	437	3.3%
Braced steel frame	SF2	3	0.0%
Metal column frame with wood, metal sheet or mesh as infill	SF3	367	2.7%
Timber	T	11	0.1%
Precarious systems	NE	148	1.1%
Not available	N/A	2379	17.7%
TOTAL		13412	100

The third structural system commonly used for schools, in El Salvador, is the one composed by RC frame with Masonry Walls without seismic gap (fully integrated), without short column geometry, in one direction and RC frame with Masonry Walls without seismic gap with short column geometry in the perpendicular direction, named RC3 with 3.7 % of the building population. The RC3 type was started to be used after de 2001 earthquakes and It was in response of the catastrophic effects produced by those ground motions on old school buildings. The RC3 type was never been subjected to any strong shaking; therefore, this building category will be study more deeply.

Table 2. shows a further categorization of the RC3 buildings by story number, seismic level and diaphragm behavior. In general terms, most of the RC3 schools have between 2 to 4 stories and have rigid floor diaphragm and flexible roof. Almost half of these structures presents a medium seismic design.



Table 2 – RC3 school buildings categorized by story number, seismic level and diaphragm behavior

Story number		Seismic Design Level		Diaphragm behavior	
Story	%	Level	%	Behavior	%
1	5.6	No Seismic Design	9.7	Rigid Floor + Flexible Roof	90.7
2-4	93.5	Low Seismic Design	47.0	Rigid Floor + Rigid Roof	3.6
+5	0.8	Medium Seismic Design	43.3	Rigid Roof	5.6

3. Input ground motions

Although El Salvador is a highly seismic country it does not possess a wide catalog of ground motion records, or a group of events that can be taken as “characteristic earthquakes”. The country is affected by two main sources of seismicity. Large but distant events that occurs along the Middle American Trench where the subducted Cocos plate is converging with the Caribbean plate. The second source of seismicity is a zone of upper crustal earthquakes with shallow foci and small-to-medium magnitudes which coincide with the main population centers.

Table 3 illustrates the main parameters of the strong motions currently available, in El Salvador, including both far and near field events. Some seismic values are presented in Table 4.

Table 3 – Main parameters of the strong motions currently available

Event	Magnitude	Main data	Network	# of stations
June 19 th , 1982 (Subduction)	$M_w = 7.3^a$	Time: 06:21 GMT Epicenter: 13.32°N 89.39°W Depth: 73.0 km	CIG	1
October 10 th , 1986 (Local)	$M_w = 5.7^b$	Time: 17:49 GMT Epicenter: 13.67°N 89.20°W Depth: 8.0 km	CIG	6
January 13 th , 2001 (Subduction)	$M_w = 7.6^c$	Time: 17:33 GMT Epicenter: 13.05°N 88.66°W Depth: 60.0 km	CIG UCA	15 10
February 13 th , 2001 (Local)	$M_w = 6.6^d$	Time: 14:22 GMT Epicenter: 13.64°N 88.94°W Depth: 13.0 km	CIG UCA	9 9
February 17 th , 2001 (Local)	$M_l = 5.1^e$	Time: 20:25 GMT Epicenter: 13.66°N 89.25°W Depth: 5.1 km	CIG	5
April 10 th , 2017 (Local)	$M_l = 4.8^a$	Time: 17:54 GMT Epicenter: 13.77°N 89.15°W Depth: 10 km	MARN	1

a: MARN (Ministry of environment and natural resources)

b: (CIG, USGS) (October 27th, 1986)

c: (USGS) (August 21st, 2001)

d: (CIG) (June 15th, 2001)

e: (CIG) (May 5th, 2001)

CIG: Centro de Investigaciones Geotécnicas (non-existent)

UCA: Universidad Centroamericana José Simeón Cañas



Table 4 – Seismic values of the strong motions currently available

Network	Event	Location	Direction:		Horizontal 1		Direction:		Horizontal 2		
			PGA (cm/seg ²)	AI (m/seg)	MSA (g)	PP (seg)	PGA (cm/seg ²)	AI (m/seg)	MSA (g)	PP (seg)	
Centro de Investigaciones Geotécnicas (CIG)	19-jun-82	Observatorio	183.8	1.98	0.75	0.79	166.7	1.46	0.75	0.68	
	10-oct-86	Centro de Investigaciones Geotécnicas	411.7	1.69	1.51	0.66	-680.8	2.49	1.98	0.26	
		Hotel Camino Real	338.7	0.98	1.59	0.46	421.1	0.89	1.11	0.50	
		Hotel Sheraton	213.9	0.36	1.04	0.24	295.6	0.58	0.72	0.56	
		Instituto Geográfico Nacional	-524.5	2.25	1.57	0.40	391.7	1.09	0.89	0.84	
		Instituto de Vivienda Urbana	379.8	0.69	0.91	0.20	667.8	1.73	1.62	0.54	
		Universidad UCA	-374.1	1.26	1.38	0.48	408.8	1.22	1.13	0.56	
	13-ene-01	Acajutla CEPA	-106.0	0.25	0.29	1.04	95.9	0.23	0.28	0.34	
		Ahuachapan	-210.0	0.62	0.59	0.36	-143.0	0.61	0.57	0.56	
		CESSA Metapan	-12.4	0.00	0.04	0.38	-13.6	0.00	0.03	0.10	
		Ciudadela Don Bosco	-245.0	0.81	0.84	0.40	-221.0	1.18	0.70	0.26	
		Cutuco	77.7	0.12	0.20	0.28	-76.3	0.15	0.23	0.26	
		Observatorio	419.5	3.85	1.54	0.40	-372.0	2.51	1.28	0.16	
		Presas 15 de Septiembre	-183.0	0.70	0.90	0.24	149.0	0.49	0.53	0.46	
		Relaciones Exteriores (F)	204.0	0.76	0.77	0.42	205.0	0.68	0.81	0.42	
		Relaciones Exteriores (S)	317.1	2.14	1.23	0.30	-298.0	1.91	1.38	0.42	
		San Miguel	118.0	0.53	0.43	0.24	133.0	0.56	0.46	0.18	
		Santa Ana	-83.6	0.15	0.29	0.86	-133.0	0.28	0.42	0.98	
		Santa Tecla	-587.7	6.35	2.48	0.16	761.0	7.72	2.76	0.32	
		Santiago de María	-702.0	11.75	3.62	0.10	-864.0	9.63	3.19	0.18	
		Seminario San José de La Montaña	267.0	1.14	0.94	0.16	247.0	1.12	0.89	0.16	
		Sensuntepeque	-59.6	0.13	0.21	0.28	80.6	0.16	0.23	0.32	
		Viveros de DUA	-301.0	0.93	1.18	0.20	-305.5	0.92	0.98	0.32	
		13-feb-01	Centro de Investigaciones Geotécnicas	69.1	0.05	0.22	0.48	-135.3	0.15	0.36	0.44
	Ciudadela Don Bosco		92.1	0.09	0.30	0.26	-98.1	0.13	0.30	0.24	
	Observatorio		-101.9	0.20	0.39	0.20	104.7	0.14	0.34	0.20	
	Presas 15 de Septiembre		25.9	0.01	0.09	0.26	19.2	0.01	0.07	0.20	
	Relaciones Exteriores (F)		41.9	0.02	0.11	0.46	-41.9	0.02	0.15	0.28	
	Relaciones Exteriores (S)		-62.3	0.05	0.21	0.16	57.1	0.05	0.24	0.28	
	Santa Tecla		-40.8	0.03	0.13	0.12	37.8	0.03	0.11	0.44	
	Seminario San José de La Montaña		69.9	0.07	0.35	0.44	64.1	0.06	0.32	0.42	
	Universidad UCA		57.4	0.06	0.25	0.22	-	-	-	-	
	Viveros de DUA (F)		38.8	0.03	0.17	0.38	40.3	0.02	0.14	0.12	
	Viveros de DUA (S)		58.2	0.08	0.27	0.42	-75.8	0.07	0.27	0.38	
	17-feb-01	Centro de Investigaciones Geotécnicas	170.9	0.12	0.68	0.14	-147.8	0.10	0.56	0.08	
		Ciudadela Don Bosco	64.4	0.01	0.25	0.12	78.3	0.02	0.31	0.10	
		Observatorio	-192.3	0.18	0.68	0.10	182.4	0.16	0.49	0.22	
		Universidad UCA	-127.3	0.07	0.41	0.20	-	-	-	-	
		Viveros de DUA (F)	69.7	0.02	0.19	0.10	72.7	0.03	0.34	0.12	
	Viveros de DUA (S)	-124.9	0.07	0.42	0.24	95.2	0.05	0.35	0.16		
	10-abr-17	Hotel Crown Plaza	292.3	0.41	1.08	0.12	303.1	0.51	1.24	0.14	
	Universidad Centroamericana José Simeón Cañas (UCA)	13-ene-01	Armenia	587.8	3.35	1.73	0.72	-444.8	4.15	1.45	0.64
			Berlin	-449.5	2.94	1.58	0.29	-361.3	3.60	1.51	0.29
			Externado	-295.0	1.15	1.11	0.50	272.0	1.05	0.78	0.50
			Panchimalco	-172.3	0.55	0.92	0.22	-149.9	0.26	0.52	0.30
San Bartolo			-153.4	0.86	0.63	0.77	194.8	1.00	0.70	0.81	
San Pedro Nonualco			563.2	5.85	2.25	0.43	-478.3	6.92	2.12	0.31	
Santa Tecla			481.1	3.16	1.91	0.55	475.0	3.44	1.88	0.51	
Tonacatepeque			-242.0	1.82	0.81	0.48	-229.5	1.69	0.84	0.43	
Zacatecoluca			-254.8	1.64	1.09	0.24	247.7	1.43	0.99	0.16	
13-feb-01		Armenia	-28.1	0.03	0.09	0.44	25.8	0.02	0.11	0.25	
		Berlin	31.4	0.04	0.15	0.77	-69.0	0.11	0.24	0.58	
		Externado	121.3	0.19	0.44	0.56	-50.9	0.04	0.13	0.38	
		Panchimalco	181.1	0.17	0.46	0.24	43.6	0.03	0.15	0.24	
		San Bartolo	104.2	0.34	0.37	0.96	120.5	0.19	0.35	0.47	
		Santa Tecla	46.5	0.04	0.16	0.85	-22.4	0.01	0.06	0.61	
		Tonacatepeque	-338.1	1.60	0.98	0.52	-234.6	0.74	0.61	0.30	
		Zacatecoluca	-400.3	1.18	0.99	0.33	255.1	0.89	1.09	0.21	

PGA: Peak ground acceleration
 AI: Arias Intensity
 MSA: Maximum Spectral Acceleration
 PP: Predominant Period



After analyzing the seismic parameters from all records and the onsite effects of each event, 11 pairs of ground motion were selected which are shown in Table 5.

Table 5 – Selected ground motions to be used on the IDA's

Event	Network	Station
October 10 th , 1986	CIG	IGN: Instituto Geográfico Nacional CIG: Centro de Investigaciones Geotécnicas HCRS: Hotel Camino Real UCA: Universidad Centroamericana "José Simeón Cañas"
January 13 th , 2001	CIG	STM: Santiago de María STC: Santa Tecla
	UCA	ARM: Armenia SPN: San Pedro Nonualco
February 13 th , 2001	UCA	TON: Tonacatepeque ZAC: Zacatecoluca
April 10 th , 2017	UCA	CRW: Hotel Crown Plaza

4. Analysis model

4.1 Building description

The a typical RC3 building has different load bearing systems in each direction. Along the transverse direction, the RC3 structure has a dual system composed by RC moment resisting frames encasing strong reinforced masonry walls every other axis. Although frames and walls work as a unity, detailing of the frames are such that have been over designed to support lateral, or seismic, actions by themselves. Along the longitudinal direction, lateral and gravity loads are resisted by RC moment resisting frames with infill masonry walls which could, or not, be detached from the RC frames, a practice that could produce short column effect. This direction will be considered as the weak, or critical, direction. RC3 buildings are two story structures with a rigid diaphragm at the second level and a flexible diaphragm at the roof level. Figures 1 and 2 illustrate a typical six span configuration along the longitudinal direction.

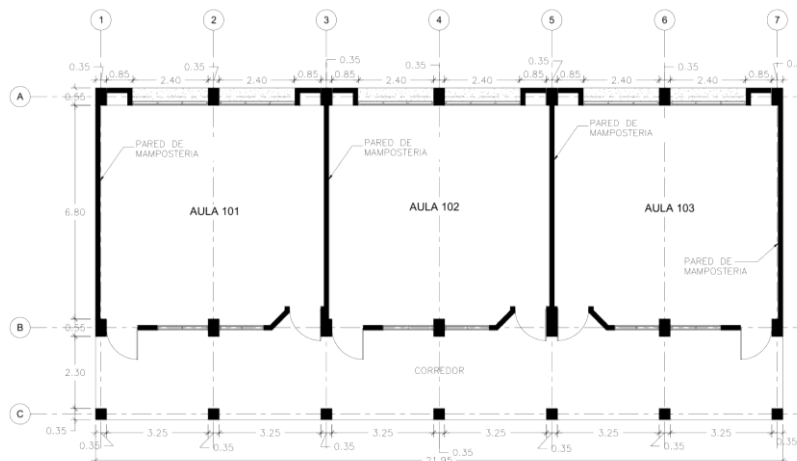


Fig. 1 – RC3 building, plan view.

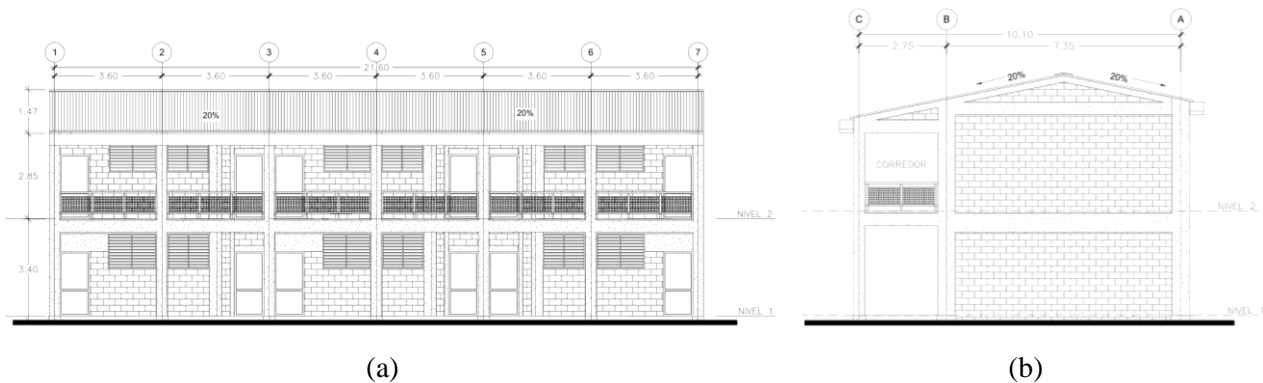


Fig. 2 – (a) RC3 building, longitudinal direction, (b) RC3 building, transverse direction.

4.2 Materials

- Structural concrete: a normal volumetric weight with strengths between 20.7 MPa (3ksi, 210 kg/cm²) and 27.6 MPa (4 ksi, 280 kg/cm²).
- Reinforcement steel: ASTM A615 with yield strengths between 275 MPa (40 ksi, 2800 kg/cm²) and 415 MPa (60 ksi, 4200 kg/cm²).
- Concrete blocks: These elements should comply with the ASTM C90 standard.

4.3 Variants

A vulnerability analysis of structures using fragility and vulnerability curves needs to consider variants that can be present in the universe of the studied typology. It was observed that the RC3 buildings does not present notable variations in geometrical configuration but in the mechanical properties of the materials.

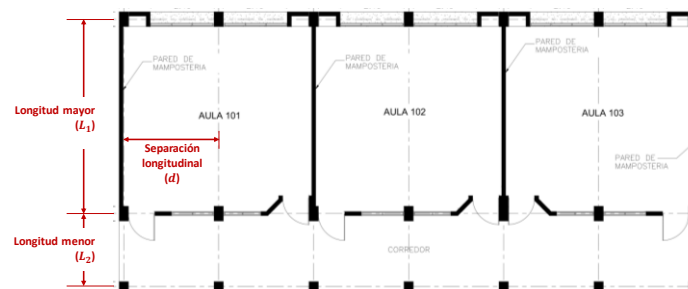


Fig. 3 – RC3 building, geometrical parameters.

The largest span (Longitud mayor) was taken as 7.00 m, the shorter span (Longitud menor) was equal to 2.80 m, the storey height was considered as 3.25 m, spans between columns (Separación longitudinal) 3.60 m. Two room configurations were used: four and six longitudinal classrooms (an example of three-room longitudinal configuration is shown in Figure 3).

For each room configuration two distinct f'_c are employed: 20.7 MPa and 27.6 MPa; and for each concrete strength, two yield strengths of the reinforcement steel are considered: 275 MPa and 415 MPa.

In summary, eight analytical models were created to which 11 pairs of ground motions are applied making 88 models to be employed in the Incremental Dynamic Analysis.



4.4 Model parameters and criteria

Mander et al. nonlinear concrete model is used to account for the behaviour of both unconfined and confined concrete materials. Whilst, the steel reinforced bars are modelled through the Menegotto-Pinto steel model. An inelastic infill panel element, which has been calibrated with the results from lab tests, has been employed to model the infill masonry.

The increment capacity due to the confinement in beams and columns due to the transverse reinforcement has been considered by means of the equations proposed by Mander, Priestly and Park, 1988.

The nominal shear strength in columns and beams has been computed using the formulae contained in the ACI318.

The load combinations, used in this research, are those proposed in the FEMA P-58-2 (Federal Emergency Management Agency, 2009), therefore:

$$1.00 D + 0.25 L \quad (1)$$

Rayleigh damping is used considering the first representative modes of vibration of each model and a damping equal to 5% of the critical in both cases.

SeismoStruct 2018 (SeismoSoft, 2018) is used to run both the static pushover and dynamic incremental analyses. A typical model is shown in Figure 5.

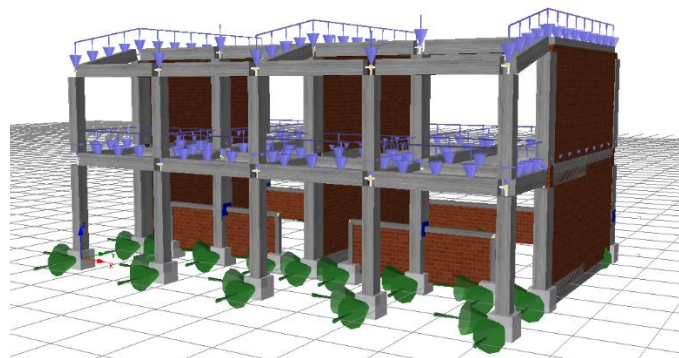


Fig. 5 – An example of the mathematical model

5. Fragility and vulnerability

5.1 Engineering demand parameters (EDP's)

Various procedures can be found in the literature to define the Engineering Demand Parameters (EDP's). Pondering that the structural elements are more affected by the relative displacement between two adjacent storeys during an earthquake, the maximum inter-storey drift (δ_{max}) is used as the EDP to assess the fragility and vulnerability of the studied buildings. Drift is understood as the difference between the total horizontal displacements of the above floor (Δ_i) and the inferior floor (Δ_{i-1}) divided by the inter-storey height (h_i).

$$\delta_i = \frac{\Delta_i - \Delta_{i-1}}{h_i} \quad (2)$$

5.2 Damage state thresholds

Considering that the inter-storey drift has been taken as EDP an appropriate attribute needs to be used to define the Damage state thresholds to quantify the seismic performance of the structures. In this case, the one defined by [1] was followed, Figure 6.

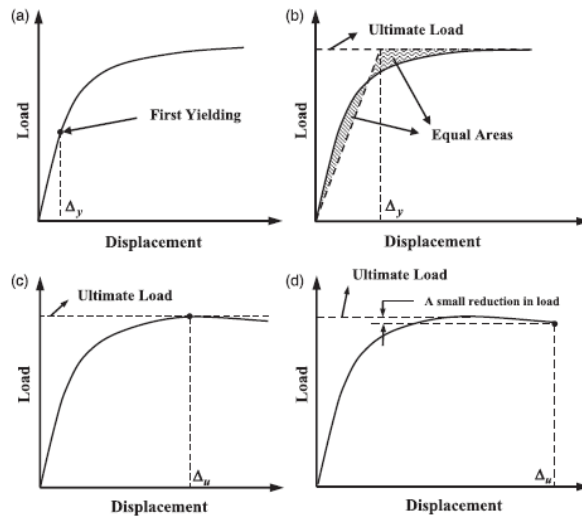


Fig. 6 – Damage state thresholds. (a) Slight (b) Moderate (c) Extensive and (d) Complete damages. Modified after [1]

Following this procedure, the slight damage threshold is assigned where the first yielding occurs, the moderate damage threshold is considered at the global yielding point, while extensive damage will be taken at the point of maximum shear and, finally, complete damage is considered when there is a 10% drop in the maximum shear.

The shape of the force vector, to perform the pushover, is proportional to the first vibration mode applied along the weak direction of the structures. The maximum inter-storey drift is identified when each damage threshold is reached, such as shown in Figure 7.

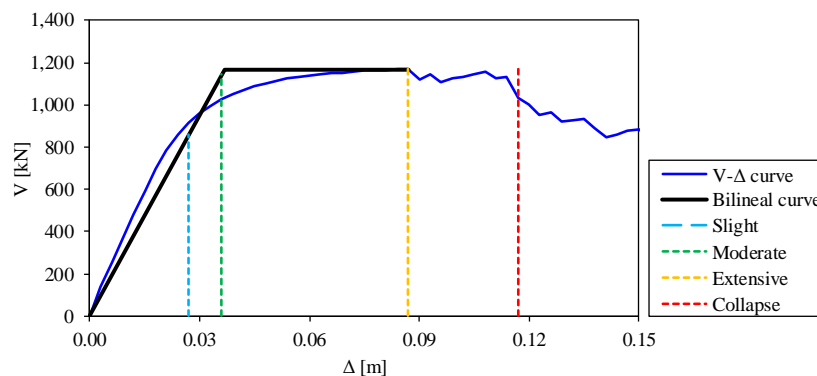


Fig. 7 – Damage state thresholds

The averages of the maximum inter-storey drifts and maximum top drifts are calculated and the results are presented in Table 7.

Table 7 – Maximum inter-storey drift and top drift averages related to each damage state thresholds

Damage state	δ_{max} (%)	
	Inter-storey drift	Top drift
Slight	0.387	0.349
Moderate	0.678	0.647
Extensive	1.434	1.271
Complete	1.703	1.606



5.3 Criteria to perform the Incremental Dynamic Analysis (IDA)

The premises to run de IDA's are as follows:

- Increments of 0.1 units up to the point of collapse have been considered. Collapse is defined as the point where there is lateral instability of the system, a soft story is formed, a drop of 10% in the lateral capacity of the structure or numerical instability is reached.
- The effect of both lateral components, acting simultaneously on the model, has been included.
- The component which has higher value of spectral acceleration at the fundamental period of the building [$Sa(T_1)$] was applied to the weak axis (understanding the weak axis as the longitudinal direction of the structure).

5.4 IDA's curves

First, maximum inter-storey drifts plotted against $Sa(T_1)$ and maximum top drifts plotted against $Sa(T_1)$ are shown in Figures 8a and 8b, respectively.

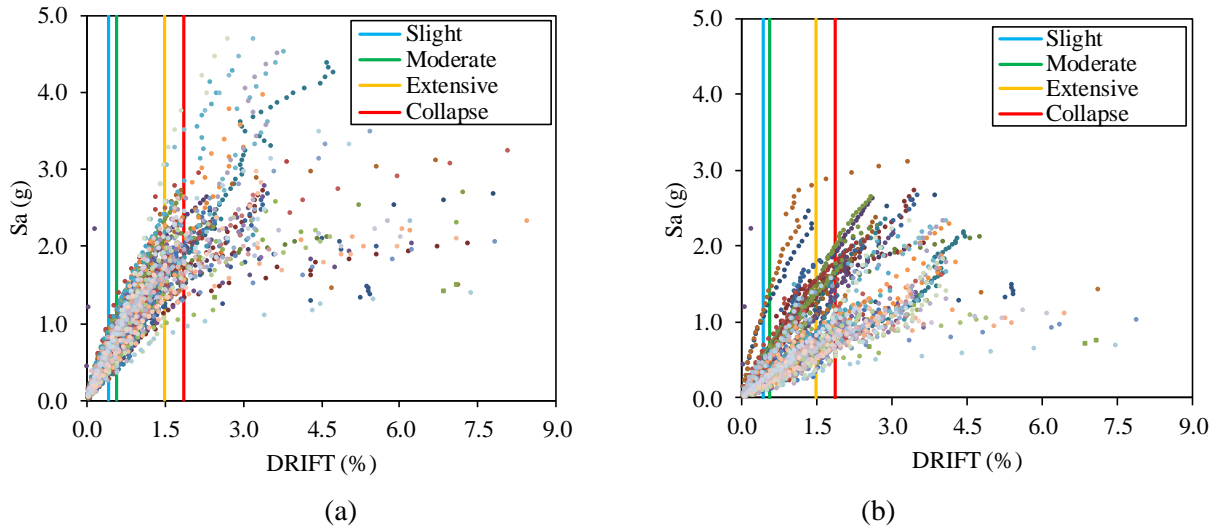


Fig. 8 – Cloud of points obtained by IDA's together with damage state thresholds (a) Maximum inter-storey drifts plotted against $Sa(T_1)$ and (b) Maximum top drifts plotted against $Sa(T_1)$

Next, the mean and dispersion at each damage state threshold is computed using the formulae proposed in [2].

$$\ln \theta = \frac{1}{n} \sum_{i=1}^n \ln IM_i \quad (3)$$

$$\beta = \sqrt{\frac{1}{n-1} \sum_{i=1}^n \left[\ln \left(\frac{IM_i}{\theta} \right) \right]^2} \quad (4)$$

Table 8 shows the parameters obtained for the four damages states using the formulae mentioned above. Maximum interstorey drift is used as EDP and $Sa(T_1)$ as the intensity measure. While, in Table 9, Maximum top drift is used as EDP and [$Sa(T_1)$] as the intensity measure.



Table 8 – Mean and dispersion for each damage state. Maximum inter-storey drifts are used as EDP and Sa(T₁) as the intensity measure.

Damage state	Parameters	
	Mean	Dispersion
Slight	0.515	0.344
Moderate	0.860	0.323
Extensive	1.656	0.266
Complete	1.804	0.250

Table 9 – Mean and dispersion for each damage state. Maximum top drifts are used as EDP and Sa(T₁) as the intensity measure.

Damage state	Parameters	
	Mean	Dispersion
Slight	0.184	0.504
Moderate	0.329	0.419
Extensive	0.581	0.450
Complete	0.825	0.485

The fragility curves are a graphical tool which relates the damage probability of a group of structures to an intensity measurement associated to the seismic demand; in the present study, the intensity measure is the spectral acceleration at the fundamental period of the structure. Using the equation (5) and the statistical parameters of Tables 8 and 9 the fragility curves depicted in Figure 9 are built.

$$P[d \geq d_i] = \Phi \left[\frac{1}{\beta_{d_i}} \ln \left(\frac{IM}{IM_{d_i}} \right) \right] \quad (5)$$

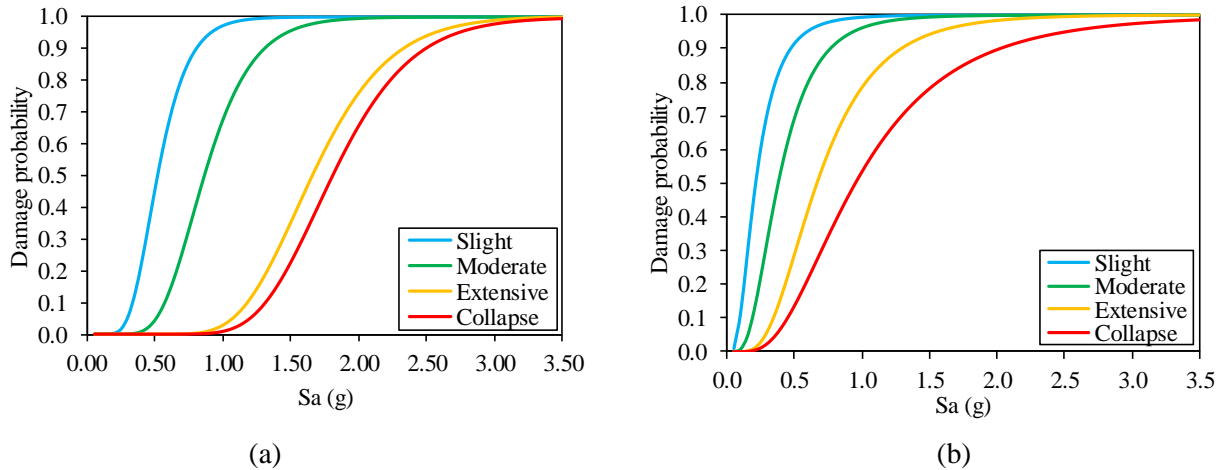


Fig. 9 – Fragility curves (a) Maximum inter-storey drifts as EDP's and [Sa(T₁)] as intensity measure and (b) Maximum top drifts plotted as EDP's and Sa(T₁) as intensity measure.

5.5 Vulnerability curves

To transform fragility curves into vulnerability curves, the formulae proposed in [3] are used, where

$$E(C > c | im) = \sum_{i=0}^n E(C > c | ds_i) \cdot P(ds_i | im) \quad (6)$$



$$\text{var}(C|im) = \sum_{i=0}^n [\text{var}(C|ds_i) + E^2(C|ds_i)]. P(ds_i|im) - E^2(C|im) \quad (7)$$

Damages ratios proposed by [4], related to the educational buildings, and presented in Table 10 are used.

Table 10 – Damage ratios.

Damage State	Damage Ratio	Var (C ds _i)
Slight	2%	0
Moderate	10%	0
Extensive	43.5%	0
Complete	100%	0

Vulnerability curves based on maximum inter-storey drifts, as EDP, and maximum top drift, as EDP are shown in Figure 10 (a) and (b), respectively.

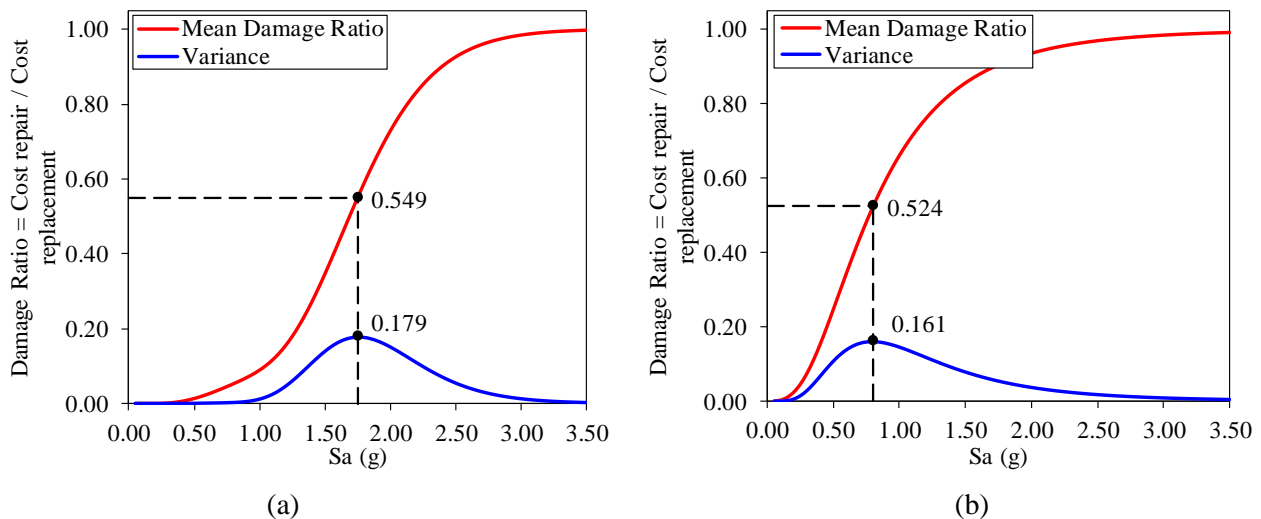


Fig. 10 – Vulnerability curves (a) Maximum inter-storey drifts as EDP's and $[Sa(T_1)]$ as intensity measure and (b) Maximum top drifts plotted as EDP's and $Sa(T_1)$ as intensity measure.

3. Conclusions

Dispersion values presented on Tables 8 and 9 are low especially when Inter-storey drift ratios are used as EDP meaning that variations on material properties, and more important, on ground motion records have a moderate effect on the computation of the fragility curves.

An important used of the fragility curves is to develop risk-targeted seismic design maps. Therefore, based on the results of the project, of which this paper belongs to, risk-targeted seismic design maps for the education infrastructure could be develop in order to project and build seismic resistant school buildings based on both the national hazard of the country and the realistic seismic behavior of the edifices.

On the other hand, the present study have developed vulnerability curves that can be used to assess the monetary loss, given a level of intensity measure, of the education portfolio in El Salvador.



4. Acknowledgements

The authors of the paper wish to acknowledge the funding provided by the World Bank, as part of the Global Program for Safer Schools (GPSS), which is an initiative of the Global Facility for Disaster Reduction and Recovery (GFDRR), to the seismic risk assessment of the education portfolio of El Salvador from which the information contained in this paper is part of.

5. Copyrights

17WCEE-IAEE 2020 reserves the copyright for the published proceedings. Authors will have the right to use content of the published paper in part or in full for their own work. Authors who use previously published data and illustrations must acknowledge the source in the figure captions.

6. References

- [1] Frankie, T.M., Gencturk, B., Elnashai, A.S. (2013): Simulation-Based Fragility Relationships for Unreinforced Masonry Buildings. *Journal of Structural Engineering*, **139** (3).
- [2] Ibarra, L. F., y Krawinkler, H. (2005): Global collapse of frame structures under seismic excitations. *PEER Project 3192002*. Pacific Earthquake Engineering Research Center.
- [3] D'Ayala, D., Meslem, A., Vamvatsikos, D., Porter, K., Rossetto, T. (2015): Guidelines for Analytical Vulnerability Assessment of Low/Mid-Rise Buildings, Vulnerability Global Component Project. DOI 10.13117/GEM.VULN-MOD.TR2014.12.
- [4] FEMA, (2003): Multi-hazard loss estimation methodology, earthquake model: HAZUS-MH MRI, technical and user's manual, Federal Emergency Management Agency, Washington, DC.
- [5] Vamvatsikos D, Cornell CA (2002): Incremental dynamic analysis. *Earthquake Engineering & Structural Dynamics*, **31** (3), 491-514.